Dynamics of Bulk Polymer Heterostructure:Electrolyte Devices

ARTICLE *in* JOURNAL OF PHYSICAL CHEMISTRY LETTERS · NOVEMBER 2010

Impact Factor: 7.46 · DOI: 10.1021/jz101405v

3 AUTHORS:

Vini Gautam
Australian National University
9 PUBLICATIONS **48** CITATIONS
SEE PROFILE

M. Bag
Indian Institute of Technology Roorkee
29 PUBLICATIONS **205** CITATIONS
SEE PROFILE

Ks Narayan
Jawaharlal Nehru Centre for Advanced Scien…
154 PUBLICATIONS **1,673** CITATIONS
SEE PROFILE

THE JOURNAL OF PHYSICAL CHEMISTRY Letters

pubs.acs.org/JPCL

Dynamics of Bulk Polymer Heterostructure/Electrolyte Devices

Vini Gautam, Monojit Bag, and K.S. Narayan*

Chemistry and Physics of Materials Unit, Jawaharlal Nehru Centre for Advanced Scientific Research, Jakkur P.O., Bangalore-560064, India

ABSTRACT The application of organic semiconductors and bulk heterojunction (BHJ) devices in photoelectrochemical cells, electrolyte-gated field effect transistors, and neuromorphic devices involves the interface of the polymer with an electrolyte. We report the observation of interesting features arising from bulk and interfacial properties of stable polymer/electrolyte devices from photovoltage and differential photocapacitance measurements. A crossover in polarity of the photovoltage signal as a function of BHJ layer thickness and a crossover in the sign of differential photocapacitance as a function of frequency are observed in certain classes of these device structures. The presence of the critical thickness and crossover frequency can be understood in the framework of an electrical transport model and the parameters defining the interfacial capacitance.

SECTION Electron Transport, Optical and Electronic Devices, Hard Matter

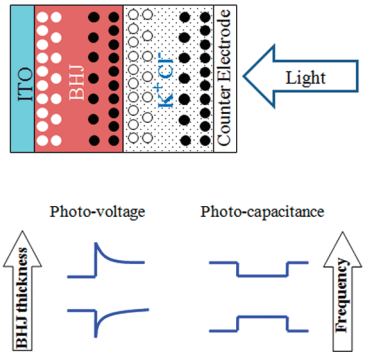

Bulk heterojunction (BHJ)-polymer-based solar cells form an extensive area of research and are rapidly emerging as possible low-cost alternatives for photovoltaic applications.[1−4] It has been found that among several limiting factors in the energy conversion process in the BHJ solar cells, the BHJ/cathode interface also plays an important role.[5,6] The interfacial kinetics and barriers significantly affect the fill factor and short-circuit current.[7] The replacement of the cathode by an electrolytic layer in the BHJ-based devices can provide valuable insight into the dynamics of the transport processes. Further, in applications such as photoelectrochemical cells[8−10] and electrolyte-gated field effect transistors,[11,12] the active polymer layer exists in contact with an electrolyte (El), and it is therefore important to understand the semiconducting polymer/electrolyte interface (PEI). Conjugated polymers have been recently used in an electrolyte-gated transistor to mimic the synaptic current or voltage pulses of the biological systems.[13] Such hybrid semiconductor/El systems have potential applications in the field of neuromorphic engineering, which involves the development of an artificial neural system whose physical architecture and design principles are based on those of biological nervous systems. Organic semiconductors like BHJs also have potential applications in hybrid tandem photovoltaic cells[14] which involve interfaces between the organic, inorganic, and electrolytic layers.[15] However, the complex nature and the stability of the conjugated polymers in contact with electrolytes are issues for the development of such devices.[16] A detailed understanding of the various interfacial layers would also be critical for the performance, efficiency, and lifetime of these device structures. The possibility of varying the thickness of the BHJ layer and the frequency (ω) in case of $C(\omega,V)$ measurements serves as a useful tool to deconvolute and estimate the different contributions in the photophysical and transport processes within these devices.

Here, we report the studies of photovoltage and photocapacitance as a function of different parameters in regioregular polyalkylthiophenes (rrP3AT)-acceptor based BHJ/El structures. We largely present results using the naphthalene-derivative-based acceptor, N2200, in the BHJ due to its enhanced stability and larger electron mobility.[17,18] We further compare the features of thiophene-derivative-based BHJ devices with those of the carbazole-derivative-based BHJ devices. The observed results highlight the role of bulk carrier concentration and diffusion length scales and the presence of different transport mechanisms prevalent in these structures. The results also provide design rules for fabrication of BHJ/El-based novel photodetectors.

A typical transient V_{ph} of the ITO|P3HT-N2200/El device structure to a wide square pulse photoexcitation is shown in Figure 1d, where the responsivity is 50 mV/mW for 1 mW, white LED incident light. It is to be noted that photoexcitation of BHJ/El device structures with KCl as the electrolyte does not result in a pure electronic current, unlike the dye-sensitized solar cells which involve an electrolyte with a regenerative redox couple like I_3^-/I^-. In the BHJ/El(KCl) structures, the response is in the form of displacement current along with a dc offset (steady-state potential) representing the ionic transport processes. We observe that for light incident from the polymer/El side, the response of BHJ/El structures with reasonably thick BHJ layers (>2 μm) is in the form of an initial positive V_{ph} spike followed by a steady-state positive potential. For light incident from the ITO side, the response is in the form of an initial negative spike followed by a near-zero

Received Date: October 13, 2010
Accepted Date: November 1, 2010

DOI: 10.1021/jz101405v | *J. Phys. Chem. Lett.* **2010**, *1*, 3277–3282

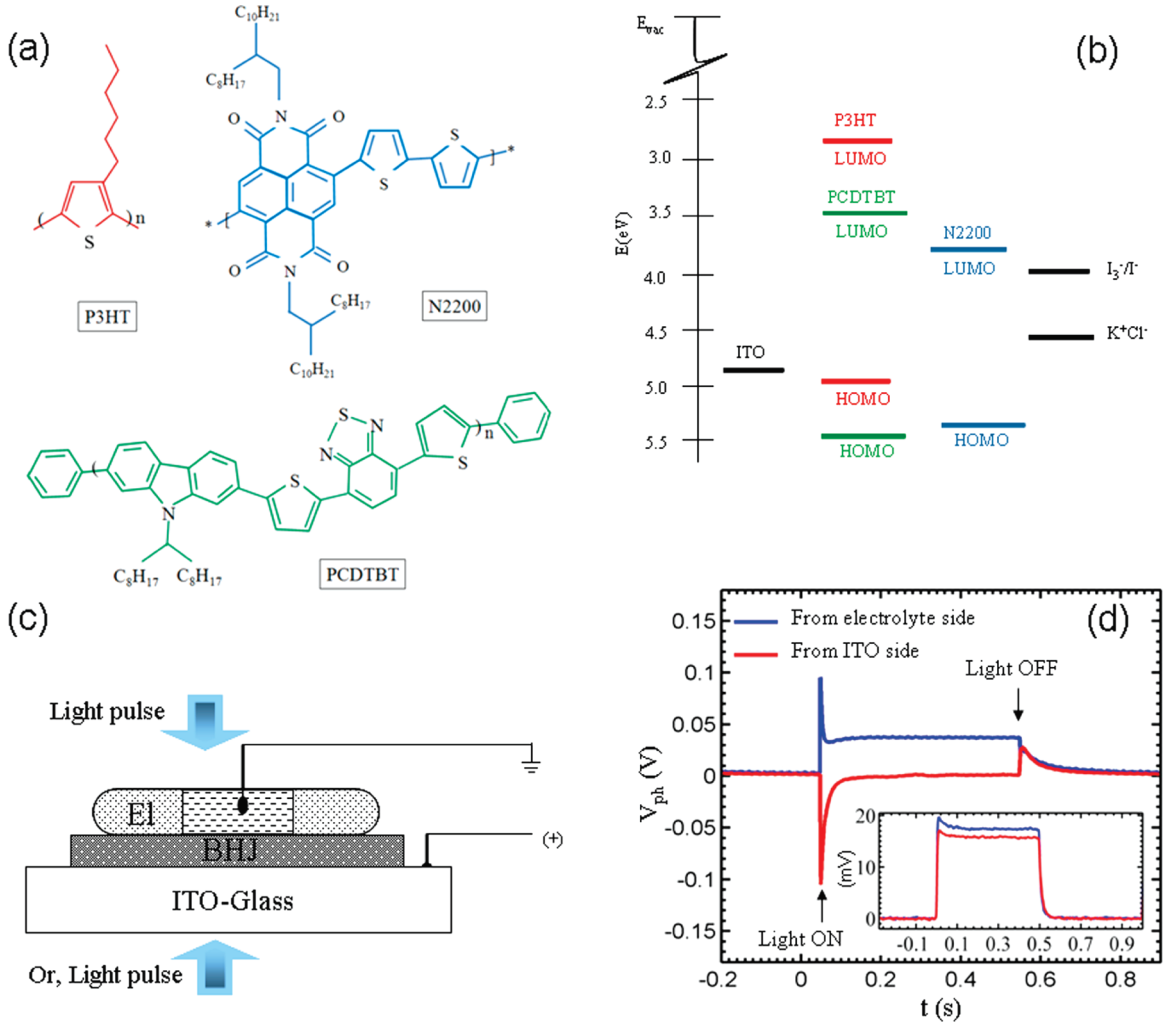

Figure 1. (a) Chemical structures of P3HT, PCDTBT, and N2200. (b) Work functions of the ITO electrode, P3HT, PCDTBT, N2200, and the electrolytes used and their relative positions with respect to the vacuum level. (c) Schematic of the measurement setup; El = electrolyte and BHJ = bulk heterojunction. (d) Device photovoltage from the P3HT-N2200 thick films (~4.5 μm) in the ITO|BHJ/El structure with KCl (100 mM) electrolyte shown for two sides of illumination. (d) (Inset) Photovoltage response of the PCDTBT-N2200 BHJ-based ITO|BHJ/El(KCl) device.

steady-state value. The photoresponse of the BHJ layer was considerably more significant compared to the case of the pristine P3HT polymer layer (Supporting Information). The incident light direction-dependent reversal of the spike polarity in V_{ph} of the thick polymer film ($> 2\,\mu$m) indicates that the active charge carrier generation region is restricted to a fraction of the total film thickness. This feature of polarity reversal with incident light direction was observed in the $400 < \lambda < 700$ nm range, which corresponds to the P3HT absorption range. However, upon replacing the donor P3HT with PCDTBT, this trend in the V_{ph} response was not observed. As shown in Figure 1d (inset), a substantially large positive V_{ph} signal is observed for the PCDTBT-N2200 based BHJ/El devices for light incident from both directions. The positive polarity of the response from the PCDTBT-based structures persisted and did not vary with the thickness and wavelength. The optical absorbance of the BHJ layer in contact with an electrolyte (Supporting Information) and the device response were fairly constant over extended hours of operation.

In the case of P3HT-based BHJs, the V_{ph} displays an interesting behavior with respect to the film thickness (Figure 2a). Upon photoexcitation from the polymer/El side, the photoresponse of a reasonably thick film (~4.5 μm) is in the form of a positive V_{ph} spike followed by a steady-state value. As the film thickness is reduced, the ratio of photovoltage spike amplitude (V_{peak}) to its steady-state value (V_{ss}) decreases, and for the film thickness of ~0.2 μm, the photovoltage reverses its polarity and appears in the form of a negative spike. Upon switching off the photoexcitation, we observe a similar polarity change that indicates a complete reversal of the nature of charge carriers involved in setting up the V_{ph}. A high sensitivity of V_{peak} and V_{ss} to the film thickness (in the 200−400 nm range) is evident in Figure 2b, where the magnitude of the ratio of V_{peak} to V_{ss} ($|V_{peak}/V_{ss}|$) also demonstrates a clear crossover as a function of thickness. However, in the case of the PCDTBT-N2200/El system, the polarity crossover as a function of thickness is not observed in the V_{ph} response (Figure 2a (inset)).

DOI: 10.1021/jz101405v | J. Phys. Chem. Lett. 2010, 1, 3277–3282

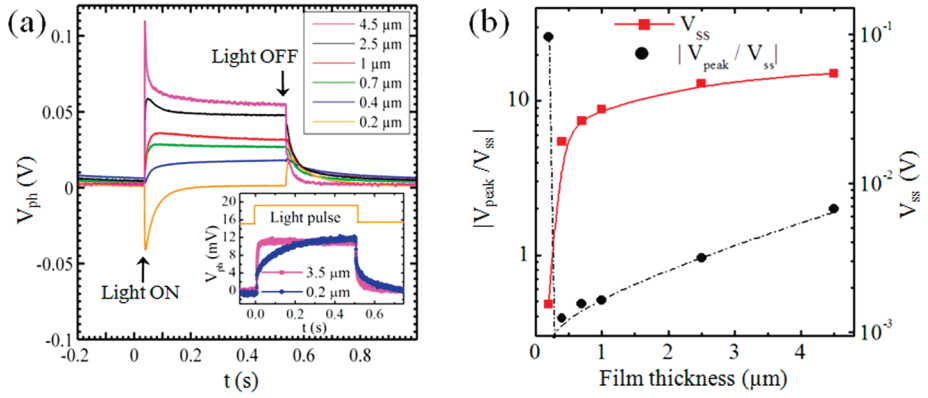

Figure 2. (a) Photovoltage response of ITO|P3HT-N2200/El device structures to a wide square wave white light pulse incident from the electrolyte side for different BHJ layer thicknesses. (a) (Inset). Photovoltage response of the ITO|PCDTBT-N2200/El device structure to a similar light pulse for BHJ layer thicknesses of 3.5 and 0.2 μm, depicting no reversal in polarity. (b) Ratio of the magnitude of the photovoltage spike (V_{peak}) to the steady-state potential (V_{ss}) and V_{ss}, as obtained from (a), as a function of film thickness.

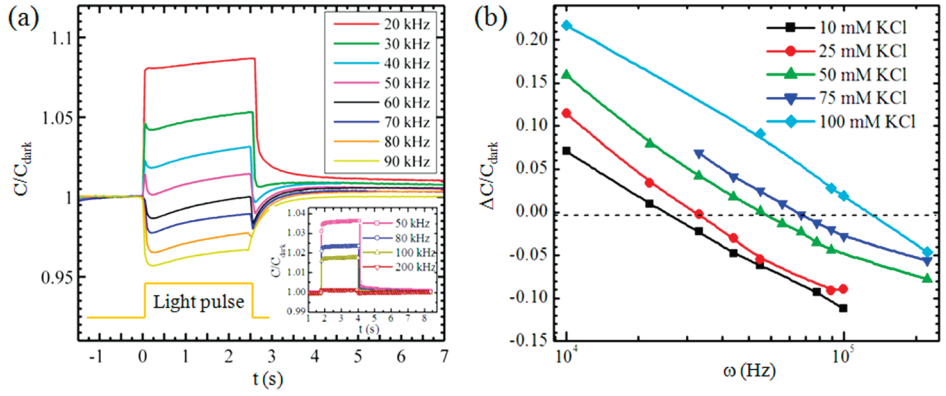

Figure 3. (a) Photocapacitance observed for the ITO|P3HT-N2200/El structure at different ω. (Inset) Photocapacitance observed for ITO|PCDTBT-N2200/El structures; 100 mM KCl is used as the electrolyte for both cases. (b) Differential photocapacitance $\Delta C/C_{dark}$ obtained from (a), plotted as a function of ω for various electrolyte concentrations.

Using differential $C(\omega)$ measurements over a large ω range (10 kHz to 1 MHz), we observe the existence of a crossover ω in BHJ/El structures beyond which the electrolyte properties dominate the device characteristics. In general, $C(\omega)$ of BHJ/El-based devices monotonically decreases with increasing ω in the 10 kHz to 1 MHz range (Supporting Information). Photoexcitation of the P3HT-N2200-based BHJ/El structure results in a change of $C(\omega)$, where at low ω, $C_{light} > C_{dark}$ and at high ω, $C_{light} < C_{dark}$, as shown in Figure 3a. The differential photocapacitance $\Delta C/C_{dark}$, where $\Delta C = C_{light} - C_{dark}$, is observed to change from a positive to negative value as ω is increased from 10 kHz to 1 MHz (Figure 3b). The magnitude of the critical frequency (ω_c), which corresponds to the polarity change of $\Delta C/C_{dark}$, is dependent on the following factors: (i) ω_c is observed to shift to the higher magnitude as the charge generation and transport efficiency of the BHJ layer increase, as observed in the case of more efficient PCDTBT-N2200 (Figure 3a (inset)) in comparison to P3HT-N2200 BHJ/El structures or pristine P3HT/El structures (Supporting Information); (ii) ω_c increases with increasing film thickness 200 nm $< x <$ 2 μm) (Supporting Information); and (iii) ω_c increases with the electrolyte concentration (10−100 mM) (Supporting Information).

Considerable insight into the ω dependence is obtained from $C-V$ measurements. Since the analysis of $C-V$ is less complex for the unipolar pristine systems compared to that for the ambipolar BHJs, we highlight the trend of $C(V)$ at different ω for P3HT/El structures (Figure 4). At low ω (around 10 kHz), the $C-V$ curve follows the expected curve for a p-type semiconductor, as shown in Scheme 2a. At high ω (around 100 kHz), the $C-V$ curve changes its slope in the positive bias region. There is a crossover ω at which this transition occurs, and it is found to be the same as ω_c, related to the crossover of the $\Delta C/C_{dark}$. Measurements in such high ω regimes have not been reported previously for organic semiconductors. The charge carrier concentration and flat band potential for the P3HT space charge region using the Mott−Schottky relation is estimated from $1/C^2$ versus V plots for the P3HT/El device (Supporting Information) and is consistent with those reported from low ω measurements.[19]

The essential features then arising from the measurements of the BHJ/El(KCl) structures are the following: (i) The V_{ph} spike polarity exhibits a crossover as a function of BHJ layer thickness, and (ii) $\Delta C/C_{dark}$ and $C(V)$ exhibit a crossover as a function of ω. These results can be understood by a device model which is comprised of a photoactive layer and discrete

DOI: 10.1021/jz101405v | J. Phys. Chem. Lett. 2010, 1, 3277–3282

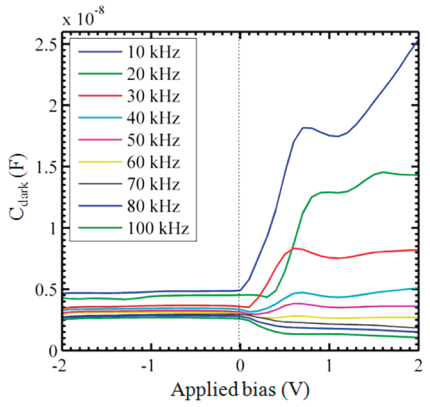

Figure 4. $C-V$ plots obtained at various frequencies ω for the P3HT/PMII polymer/El structure, under nonilluminated conditions. The slope of the plot gets reversed at high ω.

but coupled capacitive layers. The light incident direction-dependent polarity of the V_{ph} spike is controlled by the charge-transfer efficiency of the electrode/electrolyte along with the extent of photogenerated carrier diffusion. Photoexcitation of BHJ/El with thick polymer films (> 2 μm) from the electrolyte side results in the generation of charge carriers largely at the polymer/El side. The interface energetics are expected to be conducive for electron transfer from the semiconductor bulk (lowest LUMO level, −3.3 eV) to the electrolyte layer (Figure 1b), while the photogenerated holes diffuse to the ITO electrode. The large prominent spikes associated with the initial response to the photoexcitation arises from the barrier which facilitates the electron accumulation and the dynamics associated with the hole collection at the electrode. The photoexcitation of BHJ/El with thick polymer films (> 2 μm) from the ITO side results in a net positive charge accumulation at the counter electrode side relative to that at the ITO side in the form of a negative spike. In general, barriers of higher magnitude appear in the transport process induced by light incident from the ITO side compared to that from the El side.

The thickness-dependent polarity reversal of V_{ph} in P3HT-N2200 structures can be quantitatively explained by the differences in the charge-transport dynamics (electrons versus holes) accompanied by the ionic processes and expectedly is a function of thickness of the BHJ layer. The V_{ph} of a device can be estimated from the electron and hole concentrations at the ITO|polymer interface using the proposed diffusion model (Supporting Information). As shown in Scheme 1, the effective carrier concentration is dominated by holes for $x > L_c$ and by electrons for $x < L_c$, where x = the thickness of the BHJ layer and L_c = critical thickness. Further, at $x = L_c$, $V_{ph} = 0$, which implies $L_c = [\ln[(L_p\mu_n n_0^{eff})/(L_n\mu_p p_0^{eff})]/(1/L_n - 1/L_p)]$, where L_p, μ_p, and p_0^{eff} and L_n, μ_n, n_0^{eff} are the diffusion length scales, mobility, and the effective carrier concentration at the PEI at a given time (say $t = \tau_{tr}$, the transit time) for holes and electrons, respectively. Upon assuming $\mu_n n_0^{eff} \approx \mu_p p_0^{eff}$, L_c can be simplified to $L_c \approx [(L_n L_p)/(L_p - L_n)] \ln(L_p/L_n)$. The observed value of L_c is 300 nm. The presence of a finite steady-state signal which appears to plateau in samples as thick as 4−5 μm is indicative

Scheme 1. Effective Carrier Concentration at the ITO|BHJ Interface with Light Incident from the El Side and the Photovoltage Peak Value (V_{peak}) as Modeled from the Drift−Diffusion Equation (see text)

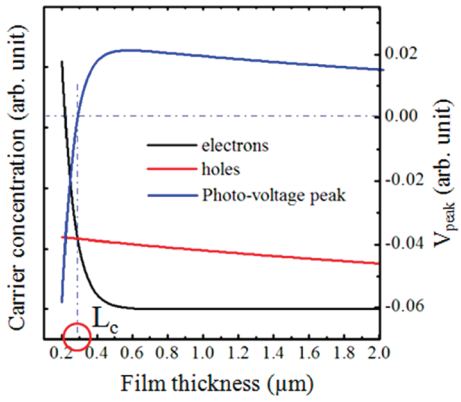

of $L_p \approx$ film thickness. This assumption in turn leads to a value of $L_n \approx 70$ nm from the above expression. The feature of thickness dependence has been utilized for demonstrating light-sensing applications in our laboratory.

It is interesting to note that in the case of PCDTBT-N2200 structures, both features of significant V_{ph} spike and polarity reversal are absent in the measured intensity and time scales. These trends largely point to a barrier-free interface in the case of PCDTBT/El compared to that of P3HT/El and can be ascribed to the lower solvent reorganization energy at the PCDTBT/El interface. Further, the response of the BHJ/El(KCl) combination is lower than that arising from a BHJ/El combination where the electrolyte constitutes a regenerative redox couple like I_3^-/I^-. As expected, the more sizable response of the BHJ/El(I_3^-/I^-) device does not have the charging signature in the form of the transient V_{ph} spike observed for KCl electrolyte devices (Supporting Information). The slower photoresponse due to the presence of ionic transport in the BHJ/El(KCl) devices obviously is not suitable for photovoltaic applications, but the significant responsivity and the thickness-dependent polarity features make this system an interesting light detector that can be used in a biological environment besides its use as a model structure for understanding the limitations and transport barriers in hybrid electronic/ionic systems.

The discontinuity in the structural phases in the BHJ/El hybrid system translates as electrical discontinuities at the PEI in a suitable ω regime. The distribution of electrons/ions at the PEI produces a space charge layer (d_{SC}) on the semiconductor side in addition to the existing Helmholtz layer (d_H) and a diffuse charge layer (d_d) on the electrolyte side, giving rise to associated capacitances C_{SC}, C_H, and C_d, respectively.[20] As shown in Scheme 2a, the total capacitance, C_T, can be expressed as a series sum of C_{SC}, C_H, and C_d, and in general, C_T follows the trend of C_{SC} along the accumulation, depletion, and deep depletion regime.[20] Upon photoexcitation of the PEI, free charge carriers (electrons and holes) originate from the exciton dissociation at the BHJ interface. The resulting charge redistribution at the PEI thereby modifies the barrier potential at the interface, which is then reflected in the interfacial capacitance magnitudes. Further, the discrete

DOI: 10.1021/jz101405v | J. Phys. Chem. Lett. 2010, 1, 3277–3282

Scheme 2. (a) Behavior of Space Charge Capacitances of a p-Type Semiconductor as a Function of Bias[20,21] and (b) C_T Following the Profile of C_H at Much Higher ω[a]

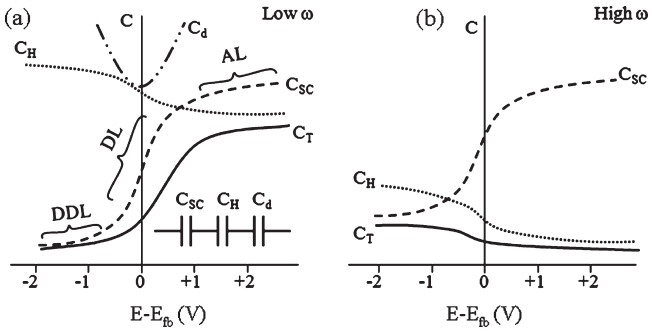

[a] C_{SC} is the space charge capacitance of the semiconductor, C_H is the Helmholtz layer capacitance, C_d is the capacitance of the diffuse layer of charges in the electrolyte, and C_T is the total capacitance. E_{fb} is the flat band potential of the semiconductor, and E is the applied bias. AL, DL, and DDL represent the accumulation, depletion, and deep depletion regimes of the space charge capacitance, respectively. At low ω, C_T follows the profile of C_{SC}.

changes in the transport mechanisms across the bulk and interfacial layers are expected to reveal characteristic features which manifest at high frequencies.

In order to explain the crossover of the $\Delta C/C_{dark}$ upon photoexcitation at ω_c, it is instructive to examine the individual functional dependence of $C_{SC}(\omega)$ and $C_H(\omega)$ in the measurement range of 10 kHz $< \omega <$ 1 MHz. The photogeneration of charge carriers in the semiconducting polymer film reduces d_{SC}, resulting in an increase in C_{SC}. At lower range ω ($< \omega_c$) where C_{SC} dominates the C_T trend, the increase in C_{SC} results in the increase in C_T upon photoexcitation, and $\Delta C/C_{dark}$ is positive. The photoillumination of PEI also generates a photopotential at the interface in a direction opposite to the existing field across the PEI.[21] The decrease in the field across the Helmholtz layer reduces the polarization of the adsorbed solvent molecules, leading to a decrease in C_H. At higher-range ω ($> \omega_c$), where C_H dominates the C_T trend,[22] the decrease in C_H upon photoexcitation therefore results in a decrease in C_T, and $\Delta C/C_{dark}$ is negative. The transition from a positive to negative value of $\Delta C/C_{dark}$ at high ω can then be attributed to the change in the dominant contributing factor to C_T. The crossover from the C_{SC} dominating behavior to that of C_H also surfaces in the $C-V$ studies of pristine P3HT-based polymer/El devices, where C_T follows the C_{SC} profile of a p-type semiconductor/El interface at low ω. At high ω, C_T follows the profile of C_H. This phenomenon of crossover is depicted in the suggested Scheme 2b, which explains the experimentally obtained trend of $C(V)$ shown in Figure 4.

In summary, $V_{ph}(t)$ and $\Delta C/C_{dark}(\omega)$ measurements provide significant insight into the photoinduced transport mechanisms of a BHJ/El structures. The interesting trend in the form of a crossover in the polarity of the initial V_{ph} spikes as a function of thickness can provide relative estimates of the macroscopic transport length scales. The crossover associated with the $\Delta C/C_{dark}$ indicates a change in the dominant contribution to the total C, with, primarily, a larger contribution from C_{SC} at low ω and from C_H at higher ω. The crossover with respect to thickness and frequency however are not observed in the case of PCDTBT-N2200-based BHJ/El devices. These results have significant implications for the choice and design of novel BHJ/El-based photodetectors.

MATERIALS AND METHODS

We have used two types of donor-type polymers, (i) poly-[3-hexylthiophene] (P3HT) obtained from Sigma Aldrich and (ii) poly-[*N*-9′-heptadecanyl-2,7-carbazole-alt-5,5-(4′,7′-di-2-thienyl-2′,1′,3′-benzothiadiazole) (PCDTBT) obtained from Konarka Inc., U.S.A. As the acceptor-type polymer, we have used poly{[*N*,*N*′-bis(2-octyldodecyl)-naphthalene-1,4,5,8-bis-(dicarboximide)-2,6-diyl]-alt-5,5′-(2,2′-bithiophene)}(N2200) obtained from Polyera ActivInk, U.S.A. All polymers were used without additional purification. Chemical structures and relative energy levels of these polymers are shown in Figure 1a,b. Blends of P3HT-N2200 and PCDTBT-N2200 are prepared in a 1:1 ratio (w/w) with chlorobenzene as the solvent (20 mg/mL concentration). The BHJ solution is drop cast onto precleaned indium−tin oxide (ITO)-coated glass substrates (20 Ω/□) for thick films (400 nm−4.5 μm), while thin films (∼200 nm) were made by spin-casting the blend solution onto the substrate at 1000 rpm speed for 100 s. All devices were fabricated inside of a glovebox (Mbraun Inc.) and cured at 80 °C for 20 min. KCl or solvent-free 3-propyl-1-methyl imidazolium iodide (PMII) was used as the electrolyte. Polydimethylsiloxane (PDMS) wells (diameter ≈ 2 mm) were used to hold liquid electrolyte on top of the polymer film. Pt-coated FTO glass or Ag/AgCl pellets were used as counter electrodes in contact with the electrolyte and were maintained at ground potential for all measurements. The thickness of the polymer films was measured using a Dektak stylus profilometer (Veeco Instruments Inc.) with a 3 mg tip force and 12.5 μm tip size. Ultrafast LEDs driven by a frequency generator (Sony Tektronix AFG320) were used as light sources. Photoillumination was from either the ITO|polymer or polymer/El side. The V_{ph} response across the ITO|polymer/El structures was recorded with a LeCroy (Waverunner6100A) oscilloscope across a 1 MΩ coupling resistor in the dc mode, while $C(\omega)$ and $C-V$ sweeps were recorded with a Keithley (SCS4200). The device schematic is depicted in Figure 1c.

SUPPORTING INFORMATION AVAILABLE

Figures S1−S8 include the V_{ph} response of pristine P3HT films, absorption spectra of BHJ films with and without electrolyte, ω dependence of the capacitance under dark and light conditions, normalized photocapacitance of pristine P3HT/El structures, parameters affecting the value of ω_c, Mott−Schottky plots of P3HT/El systems with charge carrier density and flat band potential calculations, the steady-state diffusion model for estimating V_{ph} and L_c, and a comparison of the V_{ph} arising from BHJ/El(KCl) with that of BHJ/El(I_3^-/I^-) devices. This material is available free of charge via the Internet at http://pubs.acs.org.

AUTHOR INFORMATION

Corresponding Author:

*To whom correspondence should be addressed. E-mail: narayan@jncasr.ac.in.

DOI: 10.1021/jz101405v | J. Phys. Chem. Lett. 2010, 1, 3277–3282

ACKNOWLEDGMENT We thank the Department of Atomic Energy, Government of India for partial funding. We also thank Konarka Inc. for providing the PCDTBT polymer.

REFERENCES

(1) Dennler, G.; Scharber, M. C.; Brabec, C. J. Polymer-Fullerene Bulk-Heterojunction Solar Cells. *Adv. Mater.* **2009,** *21*, 1323–1338.

(2) Liang, Y. Y.; Xu, Z.; Xia, J. B.; Tsai, S. T.; Wu, Y.; Li, G.; Ray, C.; Yu, L. P. For the Bright Future-Bulk Heterojunction Polymer Solar Cells with Power Conversion Efficiency of 7.4%. *Adv. Mater.* **2010,** *22*, E135–E138.

(3) Sariciftci, N. S.; Smilowitz, L.; Heeger, A. J.; Wudl, F. Photo-induced Eelectron-Transfer from a Conducting Polymer to Buckminsterfullerene. *Science* **1992,** *258*, 1474–1476.

(4) Gaudiana, R. Third-Generation Photovoltaic Technology — The Potential for Low-Cost Solar Energy Conversion. *J. Phys. Chem. Lett.* **2010,** *1*, 1288–1289.

(5) de Villers, B. T.; Tassone, C. J.; Tolbert, S. H.; Schwartz, B. J. Improving the Reproducibility of P3HT:PCBM Solar Cells by Controlling the PCBM/Cathode Interface. *J. Phys. Chem. C* **2009,** *113*, 18978–18982.

(6) Koch, N. Organic Electronic Devices and Their Functional Interfaces. *ChemPhysChem* **2007,** *8*, 1438–1455.

(7) Gupta, D.; Bag, M.; Narayan, K. S. Correlating Reduced Fill Factor in Polymer Solar Cells to Contact Effects. *Appl. Phys. Lett.* **2008,** *92*, 093301–093303.

(8) Licht, S. Multiple Band Gap Semiconductor/Electrolyte Solar Energy Conversion. *J. Phys. Chem. B* **2001,** *105*, 6281–6294.

(9) Sergawie, A.; Yohannes, T.; Gunes, S.; Neugebauer, H.; Sariciftci, N. S. Photoelectrochemical Cells Based on Emeraldine Base Form of Polyaniline. *J. Braz. Chem. Soc.* **2007,** *18*, 1189–1193.

(10) Yohannes, T.; Solomon, T.; Inganas, O. Polymer-Electrolyte-Based Photoelectrochemical Solar Energy Conversion with Poly(3-methylthiophene) Photoactive Electrode. *Synth. Met.* **1996,** *82*, 215–220.

(11) Ofer, D.; Crooks, R. M.; Wrighton, M. S. Potential Dependence of the of the Conductivity of Highly Oxidised Polythiophenes, Polypyrroles and Polyaniline. *J. Am. Chem. Soc.* **1990,** *112*, 7869–7879.

(12) Xia, Y.; Xie, W.; Ruden, P. P.; Frisbie, C. D. Carrier Localization on Surfaces of Organic Semiconductors Gated with Electrolytes. *Phys. Rev. Lett.* **2010,** *105*, 036802–036806.

(13) Lai, Q. X.; Zhang, L.; Li, Z. Y.; Stickle, W. F.; Williams, R. S.; Chen, Y. Ionic/Electronic Hybrid Materials Integrated in a Synaptic Transistor with Signal Processing and Learning Functions. *Adv. Mater.* **2010,** *22*, 2448–2453.

(14) Snaith, H. J.; Moule, A. J.; Klein, C.; Meerholz, K.; Friend, R. H.; Gratzel, M. Efficiency Enhancements in Solid-State Hybrid Solar Cells via Reduced Charge Recombination and Increased Light Capture. *Nano Lett.* **2007,** *7*, 3372–3376.

(15) Mora-Seró, I.; Bisquert, J. Breakthroughs in the Development of Semiconductor-Sensitized Solar Cells. *J. Phys. Chem. Lett.* **2010,** *1*, 3046–3052.

(16) Antognazza, M. R.; Ghezzi, D.; Musitelli, D.; Garbugli, M.; Lanzani, G. A Hybrid Solid−Liquid Polymer Photodiode for the Bioenvironment. *Appl. Phys. Lett.* **2009,** *94*, 243501–243503.

(17) Yan, H.; Chen, Z. H.; Zheng, Y.; Newman, C.; Quinn, J. R.; Dotz, F.; Kastler, M.; Facchetti, A. A High-Mobility Electron-Transporting Polymer for Printed Transistors. *Nature* **2009,** *457*, 679-U1.

(18) Rao, M; Ortiz, R. P.; Facchetti, A; Marks T. J.; Narayan, K. S. Studies of Photogenerated Charge Carriers from Donor−Acceptor Interfaces in Organic Field Effect Transistors. Implications for Organic Solar Cells. *J. Phys. Chem. C* **2010**, DOI: 10.1021/jp1051062.

(19) Bisquert, J.; Garcia-Belmonte, G.; Munar, A.; Sessolo, M.; Soriano, A.; Bolink, H. J. Band Unpinning and Photovoltaic Model for P3HT:PCBM Organic Bulk Heterojunctions under Illumination. *Chem. Phys. Lett.* **2008,** *465*, 57–62.

(20) Gerischer, H. The Impact of Semiconductors on the Concepts of Electrochemistry. *Electrochim. Acta* **1990,** *35*, 1677–1699.

(21) Sato, N. *Electrochemistry at Metal and Semiconductor Electrodes*; Elsevier: New York, 2003.

(22) Wang, Y. B.; Yuan, R. K.; Willander, M. Capacitance of Semicondoctor−Electrolyte Junction and Its Frequency Dependence. *Appl. Phys. A* **1996,** *63*, 481–486.

DOI: 10.1021/jz101405v | *J. Phys. Chem. Lett.* **2010,** *1*, 3277–3282